*Nigerian Journal of Technology (NIJOTECH)*
*Vol. 42, No. 4, December, 2023, pp.486 - 493*
*www.nijotech.com*

*Print ISSN: 0331-8443*
*Electronic ISSN: 2467-8821*
*https://doi.org/10.4314/njt.v42i4.9*

# SLIDING MODE CONTROL FOR GASIFIER REACTOR TEMPERATURE CONTROL

**AUTHORS:**
V. O. Ajah[1], E. T. Eke[2], K. E. Okoye[3], and E. C. Ejiogu[4,*]

**AFFILIATIONS:**
[1,4]Department of Electrical Engineering, University of Nigeria, Nsukka.
[1,2,4]African Center of Excellence for Sustainable Power and Energy Development, University of Nigeria, Nsukka.
[3]Mirai Denchi Nigeria Limited

***CORRESPONDING AUTHOR:**
Email: emenike.ejiogu@unn.edu.ng

**ARTICLE HISTORY:**
**Received:** 11 November, 2023.
**Revised:** 26 December, 2023.
**Accepted:** 29 December, 2023.
**Published:** 12 February, 2024.

**KEYWORDS:**
Robust control, Gasification, Data-driven, Modeling, Non-linear

**ARTICLE INCLUDES:**
Peer review

**DATA AVAILABILITY:**
On request from author(s)

**EDITORS:**
Chidozie Charles Nnaji

**FUNDING:**
None

## Abstract

*This paper presents a sliding mode control (SMC) design for gasifier reactor temperature control. Temperature control is a critical aspect of biomass gasification for quality syngas production. However, accurate modeling and effective control method are the major challenges of gasifier reactor temperature control. The gasification system processes are not yet well understood to model from the first principle due to the complex and nonlinear nature of the process. Also, conventional control methods such as proportional, integral, and derivative control have not been effective in controlling gasification systems. Hence, this work has used experimental data from a 500 kVA updraft gasifier reactor to develop a data-driven mathematical model. The system identification result predicts 86.36% goodness of fit on the model data and 88.26% on the validation data. Discrete time sliding mode control has been designed from the model and implemented in Simulink to investigate the performance of the control method on the gasifier. The result of the system time response shows that the controller effectively drives the temperature monotonically from 25°C to 700 °C in finite time (11.37 minutes). It also establishes a quasi-sliding motion with an ultimate band of* $\pm 1$℃ *for the remainder of the simulation time. Hence, the control technique guarantees optimal temperature control for any feedstock type which will result in higher conversion efficiency, more syngas yield, and improve syngas quality and durability of the gasifier reactor among others.*

## 1.0 INTRODUCTION

The global warming effects from fossil fuels have escalated the urgency for the world to transition to alternative energy sources [1]. This has further increased research in the area of renewable energy sources that have the potential to provide the energy needs of the globe. Solar, wind, geothermal, tidal, hydro, and biomass energy systems are some of the renewable energy sources that can replace fossil fuels [2]. Alternative energy sources have a lot of advantages over conventional sources. Some of the advantages are reduced greenhouse gas emissions, environmental sustainability, and clean energy [1]. However, some challenges are hindering the full deployment of renewable energy sources; these range from intermittency, storage requirement, land space requirement, location dependence, high initial cost, and conversion efficiency to technological challenges among others.

**HOW TO CITE:**
Ajah, V. O., Eke, E. T., Okoye, K. E., and Ejiogu, E. C. "Sliding Mode Control for Gasifier Reactor Temperature Control", *Nigerian Journal of Technology*, 2023; 42(4), pp. 486- 493; *https://doi.org/10.4314/njt.v42i4.9*

Hence, research is ongoing to develop and advance innovative technologies and infrastructures needed to drive sustainable energy sources [2], [3]. Biomass gasification is one of the new energy sources capable of contributing a large share in the global energy mix. It is a sustainable energy technology that involves thermochemical conversion of biomass materials – such as agricultural wastes, energy crops, municipal organic wastes, etc., – to synthesis gas. The quality and yield of syngas depend on a number of factors but operating temperature is the most influential because it impacts the reliability of the gasification system [4]. Uncontrolled or ineffective control method to the gasifier reactor may result in safety issues, equipment failures, increased maintenance cost, and fouling of the system. These make temperature control critical in the advancement of biomass gasification [2].

The challenges of temperature control in biomass gasification border on accurate modeling of the gasifier reactor and selection of appropriate control method for the system. Because the thermodynamic behaviour of the gasification process is not fully understood due to the complex and non-linear nature of the process; it is very difficult to accurately describe the system dynamics from an analytical point of view. This has restricted the control methods that can be applied to the system because conventional control methods such are proportional integral derivative (PID) control are not effective in the control of gasifier reactor [5], [6].

Researchers have approached the gasification process modelling problem in different ways [7], [8]. However, the bases for proper control implementation are lacking due to the complexity of the models. Attempts have also been made to proffer solutions to the gasification process control. The reports of the researchers in [9], [10] detail the different techniques used. However, these methods may be too complex to implement in physical systems, and so much software are required to verify the methods on simulation environments. Hence, these methods have not presented clear solution to practical gasification temperature control.

This work, therefore, presents a data-driven approach for modeling and sliding mode control (SMC) design for optimal temperature control of the gasification process. SMC method is a robust control technique that is insensitive to model uncertainties and bounded perturbation [11]–[14]. It is considered appropriate for the control of a complex nonlinear system like a gasification process. Sliding mode control of the continuous time system is well established in the literature, however, the continuous time SMC has chattering problem due to the high frequency of the switching function [13], [14]. Hence, it is not very practical in certain applications such as gasifier reactor control due to switching nonidealities [14]. Discrete time sliding mode control (DTSMC) on the other hand is practical and less difficult to implement because the frequency of the switching function depends on the sampling period [14]. Reducing the sampling period guarantees the application of DTSMC to any actuator.

### 1.1 Gasification Zones

Gasification is one of the sets of reactions that occur in a gasifier plant. It is a thermochemical process that occurs between $650℃ - 1100℃$ depending on the gasifier design and the feedstock type. A gasifier is a system that converts solid or liquid carbonaceous feedstock (biomass) into a gaseous fuel in the presence of a limited amount of oxygen. The gas is majorly composed of carbon dioxide, carbon monoxide$CO$, hydrogen $H_2$, methane $CH_4$, nitrogen $N_2$, and varied levels of higher hydrocarbons (tars) [15]. The gas produced from a gasifier is called synthesis gas or syngas. The heating value of syngas varies depending on the $CO/H_2$ ratio because the quantity of $CH_4$ is always very low compared to $CO$ and $H_2$. Biomass composition varies with feedstock type, the general representation is $CH_nO_m.wH_2O$, as shown in [6], [8].

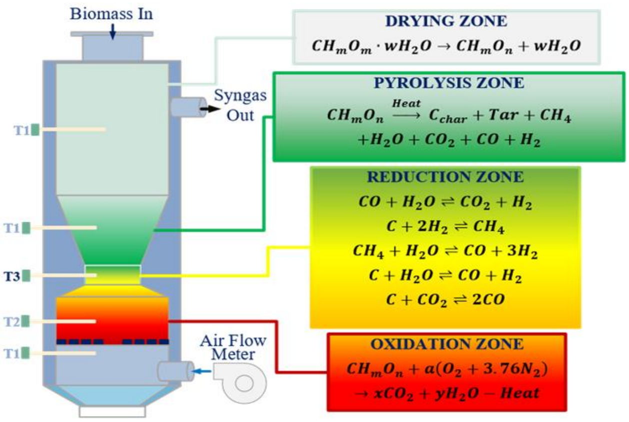


**Figure 1:** Reaction zones of gasifier Reactor

Syngas is used for power generation and also serves as feedstock for the production of other chemicals and fuels. Gasification is an alternative to conventional combustion processes and offers several advantages, such as higher efficiency and lower emissions [8]. The gasification process can be divided into four main stages or zones: drying, pyrolysis, reduction, and combustion as shown in Figure 1. The drying zone is the section where the reactions that remove moisture from the biomass feedstock take place. As the name implies, it is the removal of water from the biomass feedstock, the reactions are more visible from 100°C because of the vaporisation of water. Equation (1) is the most important reaction in the drying zone [16].

$$CH_mO_n.wH_2O \rightarrow CH_mO_n + wH_2O \quad (1)$$

The pyrolysis zone involves the decomposition of the biomass at elevated temperatures in the absence of oxygen. All the reactions of the biomass feedstocks that occur without oxygen are regarded as to have occurred in this zone. Pyrolysis converts biomass feedstock to char, bio-oil (tar), $CO, CO_2, CH_4, H_2$ and $H_2O$. Equation (2) is the common representation of pyrolysis zone reactions and occurs at the temperature range of $300℃ - 600℃$.

$$\mathbf{CH_mO_n \xrightarrow{Heat} C_{char} + Tar + CH_4 + H_2O + CO_2 + CO + H_2} \quad (2)$$

The reduction zone is where the reactions that produce the bulk of the syngas take place, hence the zone is regarded as the gasification zone. Gasification reactions are endothermic reversible reactions that occur at a temperature range of $600℃ - 1100℃$ in the presence of a limited amount of oxidizing agents. The equilibrium position of these reactions may shift to favour the forward or reverse reactions. Temperature and catalyst are the major factors that influence the equilibrium position of the gasification reactions, in the absence of catalyst (which is always the case) temperature determines the position of the equilibrium point and thus the syngas yield [8].

$$\mathbf{CO + H_2O \rightleftharpoons CO_2 + H_2} \quad (3)$$
$$\mathbf{C + 2H_2 \rightleftharpoons CH_4} \quad (4)$$
$$\mathbf{CH_4 + H_2O \rightleftharpoons CO + 3H_2} \quad (5)$$
$$\mathbf{C + H_2O \rightleftharpoons CO + H_2} \quad (6)$$
$$\mathbf{C + CO_2 \rightleftharpoons 2CO} \quad (7)$$

The oxidation zone is the source of heat for the reactions. It is the zone where combustion takes place. The heat of combustion provides all the required heat energy for the endothermic reactions of the reduction zone, the devolatilization in the pyrolysis zone, and the vaporisation in the drying zone. Equation (8) is the general representation of a combustion reaction using air as the oxidizing agent.

$$CH_mO_n + a(O_2 + 3.76N_2) \rightarrow xCO_2 + yH_2O - Heat \quad (8)$$

The mole of air $a$, required to completely burn 1 mole of dry biomass feedstock is given by Equation (9).

$$\boldsymbol{a = 1 + \frac{m}{4} + \frac{n}{2}} \quad (9)$$

## 2.0 METHODOLOGY

### 2.1 Data-driven Model

A data-driven model is a type of system identification process that uses the relationships and patterns that exit between variables in a dataset to predict the model of the system from which the dataset is created. In this work, the input variable and the system response (output variable) from experimental data are used in a black-box type of system identification to predict the model of an updraft gasifier reactor. The following steps are followed to generate the mathematical model of the fixed bed gasifier reactor.

#### 2.1.1 Experimental set-up and data collection

The experimental setup for data collection is shown in (a) of Figure 2. The set-up is an electronic interface built in the laboratory and installed on the 500kVA gasifier plant for input/output data collection. The part labelled "1" in the figure is the input and output data sensors panel. The input sensors are the input flowrate meters of the gasifier reactor and the output sensors are s-type thermocouples temperature probes installed to measure the temperature in the reactor. The sensors panel board amplifiers and digitize the weak analogue signals from the sensors and then transmit the boosted signals to the microcontroller unit. The microcontroller unit labelled "5" processes the input and output data (air flowrate and temperature values) and logs the dataset to onboard memory storage on the part labelled "4" and also displays the real-time data on the screen labelled "2".


**Figure 2:** Experimental set-up: (a) Electronic Interface (b) Thermocouple Probe and (c) Thermocouple Probe Installation

The parts of the experimental set-up labelled 1, 4, and 5 are mounted on the gasifier plant to collect and process real-time data while the part labelled 2 and 3 are mounted on a remote-control panel in the control room. The part labelled "3" and "4" have the interface that hard-wires the on-board panels and the remote panels. The 500kVA gasifier operates on an open-loop at a constant biomass feed-rate of 200kg/hr while the airflow rate varies in a step of 10kg/hr every minute, from 10kg/hr to 2000 kg/hr. The temperature of the gasification zone and the inlet air flowrate are recorded every second for 3 hours and 21 minutes. The experiment is repeated at an inlet air flowrate of 20kg/hr every minute from 100kg/hr to 500kg/hr.

The first experiment is model data while the second experiment is validation data. Temperature sensor installation on the 500kVA gasifier reactor is also shown in Figure 2. The part labelled “(b)” is the image of an s-type thermocouple temperature probe while the part labelled “(c)” shows the installation of the probe on the reactor.

#### 2.1.2 System identification

The model and validation data collection from experiment 1 and 2 are imported into the MATLAB workspace to create time domain data objects. The non-linear autoregressive exogenous (NLARX) algorithm is used in the command line environment to search and predict the lowest order (past output) that best represents the system. The predicted order is then used to configure a discrete time transfer function estimation algorithm to predict the linearized model of the system. The validation data is used to verify the goodness of fit of the predicted model.

### 2.2 Controller Design

Gasification temperature control is a tracking problem; the system state variable is expected to track reference value and remain within the limit of the predefined band. The difference between the actual system state and the reference state is the system error, $e(k) = x(k) - x_d(k)$. The objective here is to design a control input $u(k)$ that can steer the error to zero (or in the vicinity of zero, $\delta$) as the discrete time approaches infinity $\Rightarrow \lim_{k\to\infty} e(k) = 0$ or $\lim_{k\to\infty} e(k) = \delta$. The controllable canonical form state-space representation of the predicted discrete time model of the system is shown in Equation (10);

$$\begin{bmatrix} x_1(k+1) \\ x_2(k+1) \\ x_3(k+1) \\ x_4(k+1) \\ x_5(k+1) \\ x_6(k+1) \end{bmatrix} = \begin{bmatrix} 0 & 1 & 0 & 0 & 0 & 0 \\ 0 & 0 & 1 & 0 & 0 & 0 \\ 0 & 0 & 0 & 1 & 0 & 0 \\ 0 & 0 & 0 & 0 & 1 & 0 \\ 0 & 0 & 0 & 0 & 0 & 1 \\ -0.9372 & 2.182 & -0.2841 & -1.876 & -0.4423 & -2.357 \end{bmatrix} \begin{bmatrix} x_1(k) \\ x_2(k) \\ x_3(k) \\ x_4(k) \\ x_5(k) \\ x_6(k) \end{bmatrix} + \begin{bmatrix} 0 \\ 0 \\ 0 \\ 0 \\ 0 \\ 1 \end{bmatrix} u(k) \tag{10}$$

$$\mathbf{x}(\mathbf{k}+\mathbf{1}) = \mathbf{A}\mathbf{x}(\mathbf{k}) + \mathbf{B}[\mathbf{u}(\mathbf{k}) + \mathbf{d}_\mathbf{k}] \tag{11}$$

Equation (11) is the representation of the system with the disturbance term $d_k$. $x(k+1)$ is the first time-step of the state variables; $A$ is the system matrix; $(k)$ is a vector of the state variables; $B$ is the input vector and $u(k)$ is the input to the system.

#### 2.2.1 Sliding manifold design

Sliding manifold defines new dynamics for the gasifier reactor system states independent of the system parameters. The sliding manifold $s(k)$ is defined in Equation (12).

$$\mathbf{s}(\mathbf{k}) = \mathbf{M}\mathbf{e}(\mathbf{k}) \tag{12}$$

$M$ is a vector of the design parameter and $e(k)$ is states error variables.

$$\mathbf{M} = [\mathbf{m} \quad \mathbf{I}] \tag{13}$$

$m = [m_1 \quad m_2 \quad m_3 \quad m_4 \quad m_5]$ is the array of the coefficients of the characteristic equation describing the sliding manifold motion. The coefficients are so chosen (as design parameters) to ensure that the eigenvalues of the system lie within the unit circle of the z-plane and also to make $M * B$ a non-singular as well as full ranked matrix. $I$ is an identity matrix of appropriate dimension.

The sliding manifold parameters $m$ must satisfy the stability conditions (Jury’s) [14], [17] for a discrete time system. There are different methods available for the parameters design. In this work, the eigenvalue placement method is used to design the parameters.

Applying partitioned matrices to the nominal system; Equation (10) reduces it to Equation (14)

$$\begin{bmatrix} \bar{\mathbf{x}}_1(\mathbf{k}+1) \\ \bar{\mathbf{x}}_2(\mathbf{k}+1) \end{bmatrix} = \begin{bmatrix} \mathbf{a}_{11} & \mathbf{a}_{12} \\ \mathbf{a}_{21} & \mathbf{a}_{22} \end{bmatrix} \begin{bmatrix} \bar{\mathbf{x}}_1(\mathbf{k}) \\ \bar{\mathbf{x}}_2(\mathbf{k}) \end{bmatrix} + \begin{bmatrix} \mathbf{b}_1 \\ \mathbf{b}_2 \end{bmatrix} \mathbf{u}(\mathbf{k}) \tag{14}$$

Where $\bar{x}_1 \in \mathbb{R}^{5\times1}, \bar{x}_2 = \in \mathbb{R}^{1\times1}, a_{11} \in \mathbb{R}^{5\times5}, a_{12} \in \mathbb{R}^{5\times1}, a_{21} \in \mathbb{R}^{1\times5}, a_{22} \in \mathbb{R}^{1\times1}, b_1 \in \mathbb{R}^{5\times1}$ and $b_2 \in \mathbb{R}^{1\times1}$.

$$a_{11} = \begin{bmatrix} 0 & 1 & 0 & 0 & 0 \\ 0 & 0 & 1 & 0 & 0 \\ 0 & 0 & 0 & 1 & 0 \\ 0 & 0 & 0 & 0 & 1 \\ 0 & 0 & 0 & 0 & 0 \end{bmatrix}; \qquad a_{12} = \begin{bmatrix} 0 \\ 0 \\ 0 \\ 0 \\ 1 \end{bmatrix};$$

$a_{21}[-0.9372 \quad 2.182 \quad -0.2841 \quad -1.876 \quad -0.4423]$; and $a_{22} = [-2.357]$

The sliding manifold may be re-defined as shown in Equation (15):

$$\boldsymbol{\sigma} = \mathbf{M}\bar{\mathbf{x}}(\mathbf{k}) \tag{15}$$

The objective is to ensure that the sliding manifold tends to zero once sliding motion is established; therefore:

$$\sigma = 0 = m\bar{x}_1(k) + I\bar{x}_2(k) \tag{16}$$

From Equation (16), the appropriate dimension of the identity matrix I is $1 \times 1$; hence:

$$\bar{x}_2(k) = -m\bar{x}_1(k) \tag{17}$$

From Equation (17): $\bar{x}_1(k+1) = a_{11}\bar{x}_1(k) + a_{12}\bar{x}_2(k)$

$$\Rightarrow \bar{x}_1(k+1) = (a_{11} - a_{12}m)\bar{x}_1(k) \tag{18}$$

Equation (18) is a linear difference equation of a discrete time closed-loop system describing the reduced order form (new dynamics) of the system. Substituting for $a_{11}$; $a_{12}$ and $m$ in Equation (18):




https://doi.org/10.4314/njt.v42i4.9

$$\bar{x}_1(k+1) = \left( \begin{bmatrix} 0 & 1 & 0 & 0 & 0 \\ 0 & 0 & 1 & 0 & 0 \\ 0 & 0 & 0 & 1 & 0 \\ 0 & 0 & 0 & 0 & 1 \\ 0 & 0 & 0 & 0 & 0 \end{bmatrix} - \begin{bmatrix} 0 \\ 0 \\ 0 \\ 0 \\ 1 \end{bmatrix} \begin{bmatrix} m_1 & m_2 & m_3 & m_4 & m_5 \end{bmatrix} \right) \bar{x}_1(k)$$

$$\bar{x}_1(k+1) = \begin{bmatrix} 0 & 1 & 0 & 0 & 0 \\ 0 & 0 & 1 & 0 & 0 \\ 0 & 0 & 0 & 1 & 0 \\ 0 & 0 & 0 & 0 & 1 \\ -m_1 & -m_2 & -m_3 & -m_4 & -m_5 \end{bmatrix} \bar{x}_1(k) \quad (19)$$

Equation (19) is the sliding dynamics of the closed-loop system; for a completely controllable system, the poles can be placed at any desired location without altering the stability. The characteristics equation of Equation (19) is obtained by taking the determinant of $\lambda I - A_z$ (that is $|\lambda I - A_z|$); which results in Equation (20).

$$\lambda^5 + m_5\lambda^4 + m_4\lambda^3 + m_3\lambda^2 + m_2\lambda + m_1 = 0 \quad (20)$$

$\lambda$ is the poles of the new domain of the system placed along the main diagonal, $I$ is a $5 \times 5$ identity matrix,

$$A_z = \begin{bmatrix} 0 & 1 & 0 & 0 & 0 \\ 0 & 0 & 1 & 0 & 0 \\ 0 & 0 & 0 & 1 & 0 \\ 0 & 0 & 0 & 0 & 1 \\ -m_1 & -m_2 & -m_3 & -m_4 & -m_5 \end{bmatrix}$$ is the system matrix of the new domain of the system.

Placing $\lambda$ at $\lambda = [0.2 \quad 0.25 \quad 0.3 \quad 0.35 \quad 0.4]$; Equation (20) becomes Equation (21):

$$\lambda^5 - 1.5\lambda^4 + 0.8875\lambda^3 - 0.2587\lambda^2 + 0.0372\lambda - 0.0021 = 0 \quad (21)$$

Comparing Equation (20) and Equation (21):

$m = [-0.0021 \quad 0.0372 \quad -0.2587 \quad 0.8875 \quad -1.5]$

$\Rightarrow M = [-0.0021 \quad 0.0372 \quad -0.2587 \quad 0.8875 \quad -1.5 \quad 1\,]$

### 2.2.2 Control input design

The control input is designed by choosing a logical control effort that can monotonically drive the system states to the sliding manifold in finite time and maintain the system states on the manifold thereafter. It has two components: the reaching control law and the equivalent control. There are three phases of the sliding mode motion [11]. The reaching phase is when the system trajectory is driven onto the sliding manifold; the sliding phase is when the state variables are restrained and forced along the manifold toward the reference point. The last phase is the steady state phasethe , when the system has reached the reference state and the error variable has become zero (or constantly in the vicinity of zero). The first two phases are controlled by the reaching control law while the last phase is controlled by the equivalent control.

#### *2.2.2.1 The reaching law – switching control*

The reaching law is of two types: the switching reaching law and the non-switching reaching law. In this work, Goa's discrete time reaching law [14] – a switching type of reaching law – is adopted. The Goa's reaching law is shown in Equation (22).

$$s(k+1) = \alpha s(k) - \beta \operatorname{sign}(s(k)) + d(k) \quad (22)$$

The sign function is responsible for the switching characteristics of the switching reaching law, $\alpha$ and $\beta$ are the reaching law design parameters that are properly chosen to satisfy the conditions of discrete time switching reaching law [14]. $d(k)$ defines the boundedness of the system exogenous input disturbance $d_k$; this implies that $d(k) \geq |MBd_k|$.

The ultimate band (predefined band oscillation zone) $\delta$, is defined by Equation (23).

$$\delta = \frac{\beta}{1+\alpha} \quad (23)$$

$\beta > \frac{1+\alpha}{1-\alpha} d(k)$;

Taking the least upper bound of $\beta \Rightarrow \beta = sup(\frac{1+\alpha}{1-\alpha} d(k))$ and the subbing for $\beta$ in Equation (23) gives:

$$\delta = \frac{d(k)}{1-\alpha} \quad (24)$$

For $\alpha = 0; \delta \rightarrow d(k)$ which may result in system instability if $d(k)$ value is significant. For $\alpha = 1; \delta \rightarrow \infty$ which makes the system unstable. Hence, $\alpha$ is chosen between 0 and 1 to limit the width of the ultimate band.

From Goa's law of Equation (22), the switching control effort $u_{sw}(k)$, required to make the first time-step of the sliding manifold zero is given by Equation (25):

$$\mathbf{u_{sw}(k) = \alpha s(k) - \beta sign(s(k)) + d(k)} \quad (25)$$

#### *2.2.2.2 The equivalent control*

At steady-state the state variables time-steps become zero and the sliding manifold converges to zero in finite time. Hence, the sliding function in Equation (12) becomes Equation (26):

$$\mathbf{s(k+1) = 0 = Me(k+1)} \quad (26)$$

$$e(k) = x_d(k) - x(k) \Rightarrow e(k+1) = x_d(k+1) - x(k+1)$$

$$\mathbf{0 = Mx_d(k+1) - Mx(k+1)} \quad (27)$$

Putting Equation (10) into Equation (27) gives Equation (28):

$$0 = Mx_d(k+1) - M[Ax(k) + Bu(k)] \quad (28)$$

$$\mathbf{u_{eq}(k) = (MB)^{-1} M[-Ax(k) + x_d(k+1)]} \quad (29)$$

Equation (29) shows that the equivalent control operates at steady state when the disturbance has been rejected.

The control input $u(k)$ is the combination of the switching control and the equivalent control for the system with exogenous input. On the sliding manifold, Equation (22) equals Equation (26):

$$\mathbf{Mx_d(k+1) - Mx(k+1) = \alpha s(k) - \beta sign(s(k)) + d(k)} \quad (30)$$

Substituting for $x(k+1)$ from Equation (11) gives Equation (31):

$$\mathbf{Mx_d(k+1) - M(Ax(k) + B[u(k) + d_k]) = \alpha s(k) - \beta sign(s(k)) + d(k)} \quad (31)$$

From Equation (31), the control input $u(k)$, is evaluated as shown in Equation (32):

$$\mathbf{u(k)} = -(\mathbf{MB})^{-1}[\mathbf{M}(\mathbf{Ax(k)} - \mathbf{x_d(k+1)}) + \boldsymbol{\alpha}\mathbf{s(k)} - \boldsymbol{\beta}\mathbf{sign}(\mathbf{s(k)})] \quad (32)$$

The disturbance term, $d(k)$ in Goa's reaching law, has been defined as $d(k) \geq |MBd_k|$; hence, the exogenous input disturbance, $d_k$ is rejected by the switching control.

### 2.2.3 Controller implementation

Putting the control input (Equation (32)) into the nominal system (Equation (10)), the nominal closed-loop system is obtained as expressed in Equation (33).

$$x(k+1) = [I - PM]Ax(k) + PMx_d(k+1) + P[\alpha s(k) - \beta sign(s(k))] \quad (33)$$

$P = B(MB)^{-1}$

$I = 6 \times 6$ identity matrix

The simulation of the system in Simulink is carried out to study the controller performance on the gasifier reactor. The following parameters are used in the simulation:

$x(k) = [25 \quad 25 \quad 25 \quad 25 \quad 25 \quad 25]^T$ this implies that all the system state variables are at ambient temperature of $25°C$ before the gasifier is ignited.

$x_d(k) = [700 \quad 120 \quad 115 \quad 110 \quad 105 \quad 100]^T$ These is the reference state variables.

Assuming the disturbance term to be $d_k = 1.2$

$\Rightarrow d(k) = 1.167|MBd_k| = 1.4$

The reaching law parameter $\alpha$ is chosen as 0.3 and $\beta$ is estimated thus:

$\beta = 1.002 \times \frac{(1+\alpha)}{1-\alpha} \times d(k) = 2.6$

Hence, the ultimate band is calculated as 2; $\Rightarrow \delta = \pm 1$.

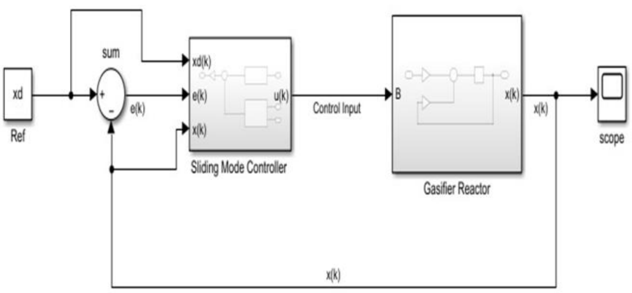


**Figure 3:** Simulink block of sliding mode control of gasifier reactor temperature

The Simulink block of the sliding mode control of the gasifier reactor temperature is shown in Figure 3. It is a closed-loop control system representing the system in Equation (33). The figure shows the reference state variables "Ref" that is compared to the actual state variables "x(k)" by the "sum" block to generate the error signal "e(k)". The reference values, error signals, and the actual state values are fed to the sliding mode controller block to compute the control effort u(k), necessary to drive the gasification temperature of the gasifier reactor towards the reference values. The process of comparing the feedback values (actual system states) to the reference states repeats until the "x(k)" equals "Ref" or is in the vicinity of "Ref". Hence, the control effort is computed to maintain the system error signal "e(k)" within the ultimate band of $\pm 1$. The reference state is the desired temperature of the gasification zone of the gasifier reactor at which a particular feedstock will produce an optimal yield of synthesis gas. For this work, the desired temperature is set to $700°C$. The system state is the actual temperature of the gasification zone which the controller has to drive from the initial value of $25°C$ to the desired value and thereafter regulate the temperature to remain in the neighborhood of the reference state as defined by the ultimate band.

## 3.0 RESULTS AND DISCUSSION

### 3.1 Model Order and Model Estimation Result

The result of the model order search with the NLARX algorithm shows 99.99% goodness of fit with six past outputs and one past input. Six past outputs mean that the reactor has characteristics of a 6th order system. TF model estimates a linear approximation of the system with one zero. The result is the discrete time transfer model shown in Equation (34). This is the mathematical description of the gasification zone in the gasifier reactor.

$$\frac{T(z)}{AF(z)} = \frac{-3.262e^{-10}z^5}{z^6 - 2.357z^5 + 0.4423z^4 + 1.876z^3 + 0.2841z^2 - 2.182z + 0.9372} \quad (34)$$

It shows 86.36% goodness of fit with the model data. The verification of the physical system representation with the validation dataset from the second experiment shows that 88.26% of the physical system is captured by the predicted model. The predicted model has been represented in the state-space controllable canonical form shown in Equation (10) and tested for controllability using MATLAB command and the result shows that the gasifier reactor is controllable. Hence, a sliding mode controller has been designed for optimal gasifier reactor temperature.

### 3.2 Controller Implementation Result for the Gasifier Reactor

The sliding mode controller implementation result is shown in Figure 4. In the figure, the blue plot, x1 is the gasification zone temperature of the gasifier reactor. The zoom-in section of the plot shows that the temperature of the gasification zone, x1 moves towards the reference temperature ($700°C$) at every sample step until it crosses the reference point and thereafter remains within the ultimate band. x1 crosses or re-crosses the reference point every sampling step.

This crossing and recrossing seeking the reference point create the zigzag motion seen in the zoom in section. The zigzag motion guarantees that the discrete time sliding motion has occurred and that x1 is in the quasi-sliding mode. The quasi-sliding is an inherent characteristic of discrete sliding mode control due to the switching between close-loop and open-loop as a result of the sampling time. At every sampling step, a certain control effort is applied to the system by the sliding mode controller. This control effort drives x1 to a certain point towards the reference (the close-loop) and then remains at that point (open-loop) until the next sampling step when another control effort is applied to the system by the controller. The dynamic behaviour of temperature in the gasification zone of the gasifier reactor under the sliding mode controller conforms with the conditions for discrete sliding mode control as stated in [14]. Hence, the sliding mode controller is effective and meets the objective of steering the error to the vicinity of zero as the discrete time approaches infinity $\lim_{k\to\infty} e(k) = \delta$. The controller drives the temperature from $25℃$ to $700℃$ in 11 minutes and 22 seconds and maintains a non-increasing oscillation amplitude of the gasifier temperature in the sliding manifold which guarantees adequate control of the optimal temperature of the feedstock in the reactor for better yield and improved syngas quality.

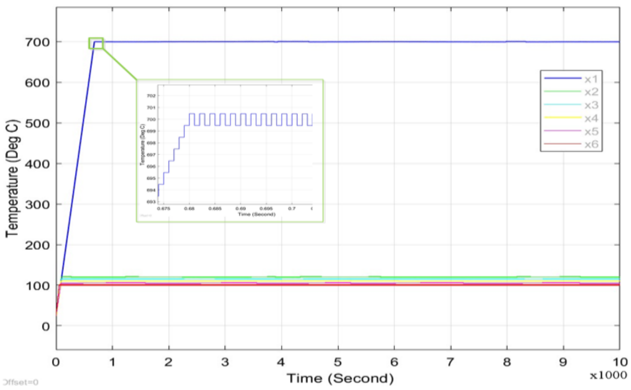


**Figure 4:** Gasifier reactor response to the sliding mode controller

## 4.0 CONCLUSION

In this paper, the sliding mode control technique has been implemented on a gasifier reactor in a Simulink environment. A data-driven modeling approach is used to develop the mathematical description of the system. The model and validation data for the modeling are from the open-loop experimental operation of a 500kVA gasifier. Gasifying air flowrates are recorded as input data and the gasification zone temperature of the reactor is output data. A 6th-order system has been predicted from the model data which shows 88.26% goodness of fit on the validation data.

The model has been used to design a discrete time sliding mode control which shows to be effective in driving the temperature of the gasification zone monotonically from ambient temperature of $25℃$ to the desired reference state of $700℃$ in finite time (11.37 minutes). The controller also maintains the temperature within the ultimate band of $\pm1℃$ for the remainder of the simulation time. The effectiveness of the controller in regulating the gasifier reactor temperature to the desired (optimal) level will result in increased conversion efficiency for the gasifier, higher syngas yield, improved syngas quality, maintenance cost savings, the durability of the gasifier reactor, reliability, safety and reduced risk in the operation.

## REFERENCES

[1] Coelho, S. T., Perecin, D., Rei, F., Escobar, J. F., Freiria, R. C., and Kimura, W. J. "Bioenergy Policies Worldwide", *Reference Module in Earth Systems and Environmental Sciences*, Jan. 2021, doi: 10.1016/B978-0-12-819727-1.00040-6.

[2] Yenugula, M., Sahoo, S. K., and Goswami, S. S. "Cloud computing for sustainable development: An analysis of environmental, economic and social benefits", *Journal of Future Sustainability*, vol. 4, no. 1, 2024, doi: 10.5267/j.jfs.2024.1.005.

[3] Srivastava, R. K. "Technical challenges and prospects of renewable fuel generation and utilization at a global scale", in *Biorefineries: Production of Fuels and Platform Chemicals*, 2024. doi: 10.1002/9781119724872.ch2.

[4] Fuchs, J., Schmid, J. C., Müller, S., Mauerhofer, A. M., Benedikt, F., and Hofbauer, H. "The impact of gasification temperature on the process characteristics of sorption enhanced reforming of biomass", *Biomass Convers Biorefin*, vol. 10, no. 4, pp. 925–936, 2020, doi: 10.1007/s13399-019-00439-9.

[5] Menmuir, D., and Hope, D. "October 2021 Advanced Gasification Technologies-Review and Benchmarking Opportunities and barriers for next generation AGTs Task 4 Report", 2021.

[6] Hussain, M., Ali, O., Raza, N., Zabiri, H., Ahmed, A., and Ali, I. "Recent advances in dynamic modeling and control studies of biomass gasification for production of hydrogen rich syngas", *RSC Advances*, vol. 13, no. 34. 2023. doi: 10.1039/d3ra01219k.

[7] P. Miguel Pereira Brito Helder Teixeira Gomes Admilson Lopes Vieira, "Modeling and simulation of biomass gasification processes Mateus Vinicius de Paiva", 2020.

[8] Perera, S. M. H. D., Wickramasinghe, C., Samarasiri, B. K. T., and Narayana, M.

"Modeling of thermochemical conversion of waste biomass – a comprehensive review", *Biofuel Research Journal*, vol. 8, no. 4, pp. 1481–1528, 2021, doi: 10.18331/BRJ2021.8.4.3.

[9] Daniel, V. P., and Gandhi, S. A. "Design for modelingand control of temperature process in downdraft gasifier system: Simulation studies", *International Journal of Pure and Applied Mathematics*, vol. 117, no. 10 Special Issue, pp. 13–17, 2017, doi: 10.12732/ijpam.v117i10.3.

[10] Dieringer, P., Marx, F., Alobaid, F., Ströhle, J., and Epple, B. "Process control strategies in chemical looping gasification-A novel process for the production of biofuels allowing for net negative CO2 emissions", *Applied Sciences (Switzerland)*, vol. 10, no. 12, 2020, doi: 10.3390/app10124271.

[11] Ajah, V., and Ejiogu, E. "Solar Thermal /Electricity Paint Curing Oven", in *1st IEEE International Conference on Sustainable Energy Technologies and Systems, ICSETS 2019*, 2019. doi: 10.1109/ICSETS.2019.8745294.

[12] Ajah, V., Ajah, G., and Ejiogu, E. "Sliding Mode Temperature Control for Hybrid Solar/Electricity Oven", vol. 10, no. 37, pp. 4654–4664, 2020.

[13] Utkin, V., Poznyak, A., Orlov, Y. V., and Polyakov, A. "Road Map for Sliding Mode Control Design", 2020. [Online]. Available: http://link.springer.com/10.1007/978-3-030-41709-3

[14] Cheng, Y.-L. *et al.*, "Discrete Time Sliding Mode Control", *Intech*, vol. 11, no. tourism, p. 13, 2016, [Online]. Available: https://www.intechopen.com/books/advanced-biometric-technologies/liveness-detection-in-biometrics

[15] Reactor, U., Gallucci, F., Sapegno, L., and Volponi, E. "Influence of Oxidant Agent on Syngas Composition: Gasification of Hazelnut Shells through an", *Energies (Basel)*, vol. 13, no. 1, p. 102, 2020, doi: doi:10.3390/en13010102.

[16] "Biomass Gasification, Pyrolysis, and Torrefaction", 2024. doi: 10.1016/c2022-0-02464-8.

[17] Ajah, V. O. "Sliding Mode Temperature Control for Hybrid Solar Thermal/Electricity Oven", Dissertation, University of Nigeria, Nsukka, 2018.